GEOLOGICA CARPATHICA, JUNE 2020, 71, 3, 221–232 https://doi.org/10.31577/GeolCarp.71.3.2

Mineralogy, geochemistry and classification of the new Smolenice iron meteorite from Slovakia

MILAN GARGULÁK[1,✉], DANIEL OZDÍN[2], PAVEL P. POVINEC[3], STANISLAV STREKOPYTOV[4,5], A.J. TIMOTHY JULL[6,7], IVAN SÝKORA[3], VLADIMÍR PORUBČAN[8] and STEFAN FARSANG[9]

[1]State Geological Institute of Dionýz Štúr, Mlynská dolina 1, 817 04 Bratislava 11, Slovakia; ✉milan@gargulak.sk
[2]Comenius University, Faculty of Natural Sciences, Department of Mineralogy and Petrology, Ilkovičova 6, 842 15 Bratislava 4, Slovakia
[3]Comenius University, Faculty of Mathematics, Physics and Informatics, Department of Nuclear Physics and Biophysics, Mlynská dolina, 842 48 Bratislava, Slovakia
[4]Natural History Museum, Imaging and Analysis Centre, Cromwell Road, London, SW7 5BD, United Kingdom
[5]National Measurement Laboratory, LGC, Queens Road, Teddington, TW11 0LY, United Kingdom
[6]University of Arizona, Department of Geosciences, Tucson, AZ 85721, USA
[7]Isotope Climatology and Environmental Research Centre, Hungarian Academy of Sciences, Institute for Nuclear Research, 4026 Debrecen, Hungary
[8]Astronomical Institute of the Slovak Academy of Sciences, Dúbravská cesta 9, 845 04 Bratislava, Slovakia
[9]University of Cambridge, Department of Earth Sciences, Downing Street, Cambridge, CB2 3EQ, United Kingdom

(Manuscript received May 6, 2019; accepted in revised form April 15, 2020; Associate Editor: Peter Bačík)

Abstract: A single 13.95 kg mass of a slightly weathered iron meteorite was found in the forest near Smolenice (48°31.2'N, 17°23.9'E; Trnava County, Slovakia). The bulk chemical composition (in wt. %) is: Fe 88.78, Ni 8.16, Co 0.38, P 0.05, S<0.006 and (in μg/g): Ge<0.18, Ir 1.67, Ga 1.80, Cr 87.3, Cu 135.1, As 4.52, Mo 5.82, Sn 1.53, W 0.56, Re 0.18, Ru 3.56, Rh 0.90, Pd 4.12, Pt 5.35, Au 1.19, Zn<5, B<0.68, Pb<0.06. Bulk geochemistry, and Ni, Ga, Ge and Ir contents in particular suggest that the meteorite is an octahedrite belonging to the IVA group. The average thickness of kamacite lamellae is 0.22 mm, ranking it as fine octahedrite (Of). The mineral composition is simple, the most abundant minerals being iron (kamacite) (5.16–7.36 wt. % Ni) followed by taenite (16.73–33.93 wt. % Ni). Troilite nodules and daubréelite inclusions and thin veinlets are rare. The Widmanstätten pattern is uniform across the meteorite and plessite structure is developed locally. Analyses of cosmogenic radionuclides (^{14}C and ^{26}Al) indicate that the radius of the Smolenice meteorite could be 30±10 cm and its terrestrial age 11±2 kyr.

Keywords: Iron, fine octahedrite (Of), IVA group, mineralogy, geochemistry, meteorite, cosmogenic radionuclides, Smolenice, Slovakia.

Introduction

The meteorite was found on 3 April 2012 during a tour in the cadastral area of Smolenice. The object had a distinct colour, shape, and density different from that of the surrounding rocks.

The Smolenice meteorite (Fig. 1) consists of a single mass of elongated shape with dimensions of 255×135×130 mm. It has a rusty colour due to the oxidation of its surface. Regmaglypts are relatively uniform across the entire surface. The mass of the recovered meteorite was 13.95 kg.

The meteorite name Smolenice was approved by the Nomenclature Committee on Meteorites at the Meteoritical Society in 2019. The main mass of meteorite is in the private collection of the finder. The type specimen is deposited in the Mineralogical Museum of Comenius University in Bratislava (24.52 g). Other samples are deposited in the Slovak National Museum – Natural History Museum in Bratislava (28.6 g and 37.9 g).

Analytical methods

Bulk chemistry

The bulk chemical composition of the meteorite was determined at the Imaging and Analysis Centre of the Natural History Museum in London. A cut piece of meteorite provided for destructive chemical analysis had a significant part of the surface covered with oxidation rind. This has been abraded by SiC sandpaper, then the fragment was rinsed and sonicated for 1 min in 2 % HNO_3, rinsed with ultra-pure (18.2 MΩ cm^{-1}) water and ethanol and dried. The pre-cleaned sample (final weight 0.73626 g) was treated with 2.5 ml concentrated HCl+2.5 ml concentrated HNO_3 (Romil SpA®) with the addition of water in a 60 ml Savillex™ fluoropolymer vessel. After leaving the vessel open at room temperature for 1 h the vessel was closed and left at 70 °C overnight. Further 3 ml HCl and 0.1 ml H_2O_2

(Merck Suprapur®) was added and the sample left closed at 70 °C for 2 h until complete dissolution. The sample was made up with water to 50 ml.

Major and minor elements (Fe, Ni, Co, and P) were determined by inductively coupled optical emission spectroscopy (ICP-OES) using a Thermo iCap 6500 Duo. Trace elements including platinum group elements (PGE) and Au were determined by inductively coupled plasma mass spectrometry (ICP-MS) using an Agilent 7700x with the collision–reaction cell (CRC) connected to He (99.9995 % purity) and H_2 (99.99999+ % nominal purity produced by H2PD-150 generator) lines. The sample solution was diluted with ca. 0.6 M HCl 20 times prior to the ICP-OES analysis and with either ca. 0.6 M HCl or with 0.45 M HCl+0.2 M HNO_3 30–60 times prior to the ICP-MS analysis and analysed 2–4 times depending on the element. Calibration standards were prepared using the same acid matrix.

Accuracy of the Co and Ni determination was verified by the simultaneous digestion and analysis of the certified reference material (CRM) BCS-251 "Low Alloy Steel". Since it is practically difficult to find a CRM close enough in composition to an iron meteorite, the accuracy of the ICP-MS analysis was checked by analysing synthetic solutions containing similar amounts of Fe and Ni with or without added analyses of interest. With the selected isotopes and the CRC modes in the ICP-MS analysis no matrix-related interferences were identified except polyatomic interferences on ^{74}Ge caused by high Fe and Ni, e.g. $^{58}Fe^{16}O$ and $^{58}Ni^{16}O$ that are not fully removable even with H_2 gas (5 ml/min) in the CRC due to extremely high Fe/Ge and Ni/Ge in the Smolenice meteorite. Therefore, we are only able to report a potential range of Ge concentrations in this meteorite.

Mineral chemistry

Electron microprobe analysis (EPMA) was carried out using a CAMECA SX100 microprobe with wavelength-dispersion spectrometers at the State Geological Institute of Dionýz Štúr in Bratislava. The operating conditions of metallic compounds were as follows: acceleration voltage of 20 keV, beam current of 20 nA and beam diameter varying from 3 to 5 μm. The following standards and lines were used for elements and sulphidic minerals: $CuFeS_2$ (Cu Kα, Fe Kα, S Kα), pure Ni (Ni Kα), pure Co (Co Kα), ZnS (Zn Kα), pure Mn (Mn Kα), pure Ge (Ge Kα), GaAs (As Lα), pure Cr (Cr Kα), pure V (V Kα), SiO_2 (Si Kα), TiO_2 (Ti Kα), Al_2O_3 (Al Kα), GaP (P Kα) and NaCl (Cl Kα). Back-scattered electron (BSE) images were conducted on the same instrument at an accelerating voltage of 15 or 20 keV with a beam current of 20 nA.

Radionuclide analyses

Gamma-ray spectrometry: Non-destructive radionuclide analyses (for gamma-ray emitters ^{26}Al and ^{40}K) were carried out in the Low-Level Gamma-Ray Spectrometry Laboratory of the Department of Nuclear Physics and Biophysics of the Faculty of Mathematics, Physics and Informatics of the Comenius University in Bratislava (Slovakia). A coaxial low-background High-purity Germanium (HPGe) detector (PGT, USA) with relative detection efficiency of 70 % (for 1332.5 keV gamma-rays of ^{60}Co) was used. The HPGe detector operated in coincidence–anticoincidence regime (with NaI(Tl) and plastic scintillator detectors) in a large low-level background lead/copper shield with outer dimensions of 2×1.5×1.5 m (Povinec 2018; Povinec et al. 2009, 2015a). A detailed description of the manual and Monte Carlo calibration procedures and applied corrections for coincidence summing effects can be found in Kováčik et al. (2012, 2013). Uncertainties of the reported results are mainly due to counting statistics. The whole uncut sample of the Smolenice meteorite (13.95 kg) was put on the HPGe detector and measured for 15 days. As we already mentioned, the meteorite was slightly weathered, typically less than 1 mm.

Accelerator Mass Spectrometry (AMS): For the ^{14}C analyses a small sample of 200 mg taken from the section of the Smolenice meteorite was used. The cosmogenic ^{14}C was extracted in a RF induction furnace in a flow of oxygen, and passing the gases evolved over a CuO furnace to ensure conversion to CO_2. This gas was collected and measured volumetrically. The CO_2 was then converted to graphite and analysed on a 3 MV AMS machine at the University of Arizona (Tucson USA). The full procedure for ^{14}C measurements is given in Jull et al. (1993, 2010).

Fig. 1. The original shape of the Smolenice meteorite. The original dimensions were 255×135×130 mm and the weight was 13.95 kg (photo: M. Gargulák).

Etching

For etching nital (15 ml 65 % nitric acid+90 ml 96 % ethanol) was used. The etching time was 1 minute and it was done at ambient temperature.

Results and interpretation

Mineral composition

The mineral composition of the Smolenice iron is simple. It is composed predominantly of iron (kamacite) and minor phases taenite, troilite, and daubréelite.

Iron (Fe, Ni) – kamacite constitutes more than 95 vol. % of the meteorite. In Smolenice five different types can be distinguished (Fig. 2):

I. Lamellae separated by a thin layer of taenite, together forming a characteristic crystal lattice of the iron meteorites (Fig. 3);
II. Lamellae usually considerably thinner than type I and terminated in finger-shaped contact (Fig. 4);
III. Allotriomorphic shapes of predominantly elongated type, sharply separated from other lamellae by thin taenite layer (Fig. 5);
IV. Matrix in which kamacite together with taenite forms a typical plessite texture (Fig. 6);
V. Matrix found between the individual lamellae without taenite (Fig. 7).

Types I and IV are the most abundant; type V is less common and types II and III are rare. The kamacite I lamellae cross in three main directions, intersecting at angles of 66±2°, 67±2° and 47±2°, 68±2°, 69±2° and 43±2° respectively. The occurrence of two groups of different angles suggests that two crystal grains were captured in a studied polished section. These two grains (the crystals) are rotated approximately 1.5° relative to each other (Fig. 8) and separated by type III kamacite lamella. The average width of the dominant type I iron lamellae in the polished section is 0.25 mm (0.11–0.39 mm, n=31); after the calculation (according to Frost 1965) with respect to the orientation of the polished section it is 0.22 mm (0.10–0.35 mm).

Neumann's lines were not observed. The measured lamellae widths correspond to iron of the fine octahedrite type (Of).

The crystal-chemical formula of kamacite is ($Fe_{0.924–0.946}Ni_{0.049–0.071}Co_{0.004–0.006}$).

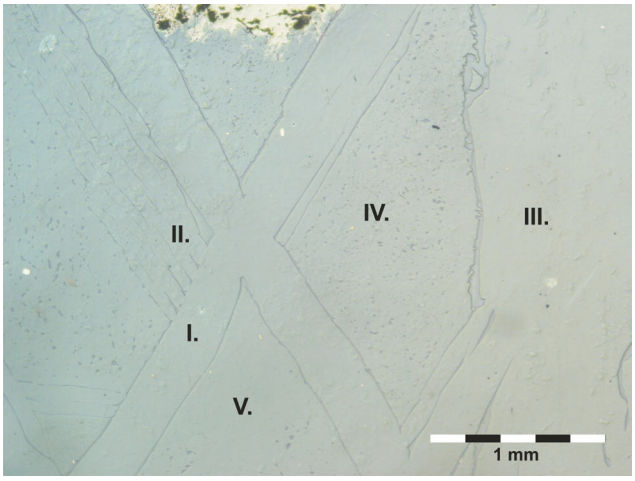

Fig. 2. Different types of kamacite (explanation in text).

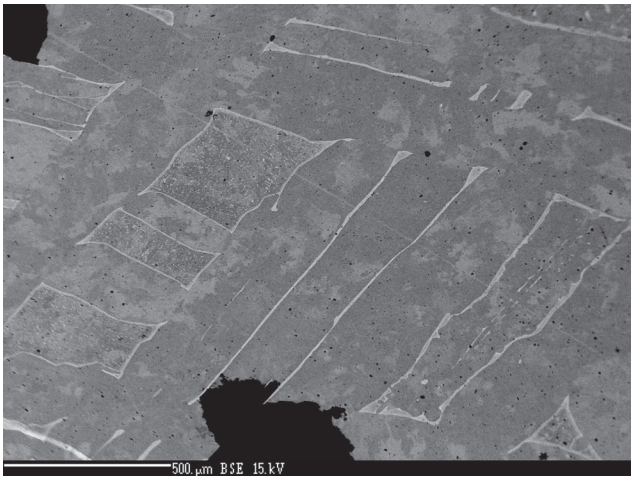

Fig. 3. Kamacite I. (BSE).

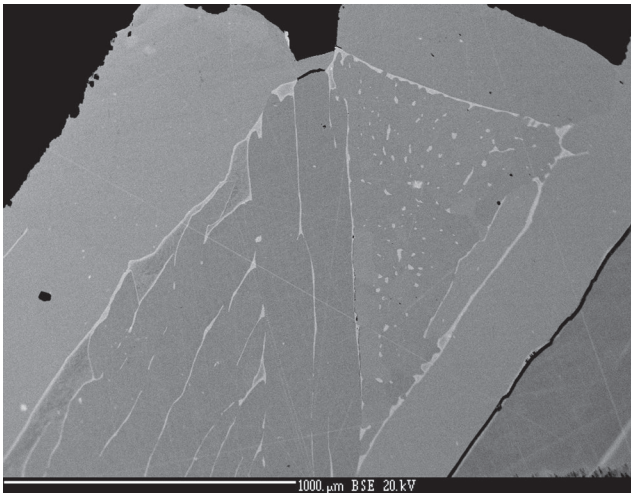

Fig. 4. Kamacite II. (BSE)

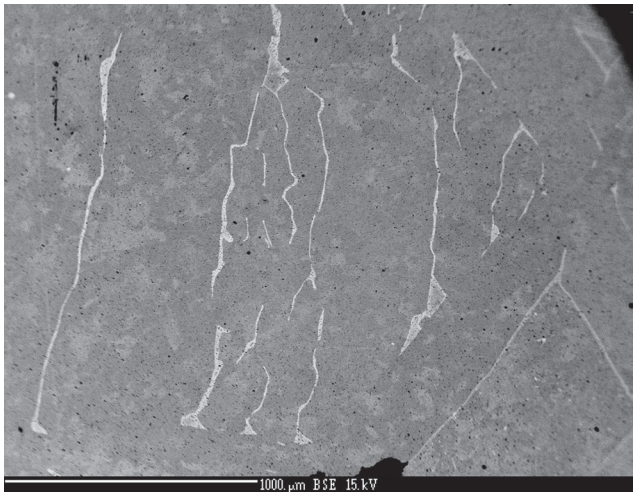

Fig. 5. Kamacite III. (BSE)

The average Ni content of the kamacite is 6.76 wt. % (5.16–7.36, n=38). Electron microprobe analyses of the kamacite are given in Table 1, except Zn, Mn, Cr, Al, Ti, V, Ga, S, Cl, which were below the detection limit.

Taenite – (Fe, Ni) is present in the two basic forms. The dominant form are thin films with a thickness of only 2.7–11.8 μm (average 7.4 μm, n=23) that separate the individual lamellae of kamacite I (Fig. 3). Less represented is the common occurrence of taenite and kamacite IV forming plessite texture. The taenite occurs in the form of allotriomorphic grains, which are approximately isometric or stretched in one direction according to the cut of the polished section. In the spaces between the parallel kamacite I lamellae, the taenite grains in kamacite IV are oriented omni-directionally and the average grain size is 19.2 μm (9.3–48.9 μm, n=24; Fig. 8a). In the spaces of the matrix enclosed by the three kamacite I oblique lamellae, the taenite grains are oriented parallel to the kamacite I lamellae and form Widmanstätten pattern (Fig. 8b). The smallest size of the taenite grains was observed in orientated plessite textures. The grains are elongated here in a direction parallel to kamacite I; their average width is 1.0 μm (0.5–1.8, n=21) and the average length is 3.7 μm (0.8–7.6, n=21).

The length–width ratio of individual grains varies from 1.1 to 13.3. In many cases, diffuse transition between taenite and kamacite IV (Fig. 6) with a gradual transition to the plessite texture can be observed at the edge of the iron lamellae.

The crystal-chemical formula of taenite is ($Fe_{0.668–0,834}Ni_{0.160–0.328}Co_{0.001–0.005}Cu_{0.000–0.002}$). The average content of Ni in taenite is 24.54 wt. % (16.73–33.93, n=38). Electron microprobe analyses of taenite are given in Table 2, except Zn, Mn, Cr, Al, V, Ti, Ga, S, Cl which were below the detection limit.

The kamacite is relatively homogeneous and its Ni content is within a narrow range of 5.16–7.36 wt. %. A dispersion of 16.73–33.93 wt. % Ni was found in the taenite, but high values characteristic for tetrataenite were not found. In both phases, a significant Fe–Ni substitution characteristic for meteoric iron was recorded (Fig. 9a). Of the other monitored elements,

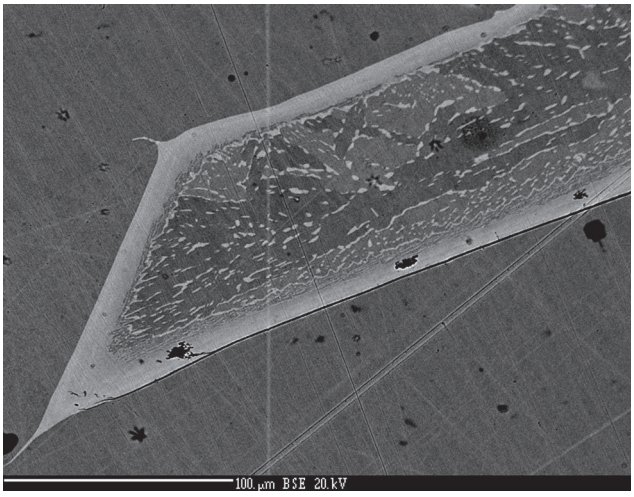

Fig. 6. Kamacite IV. (BSE)

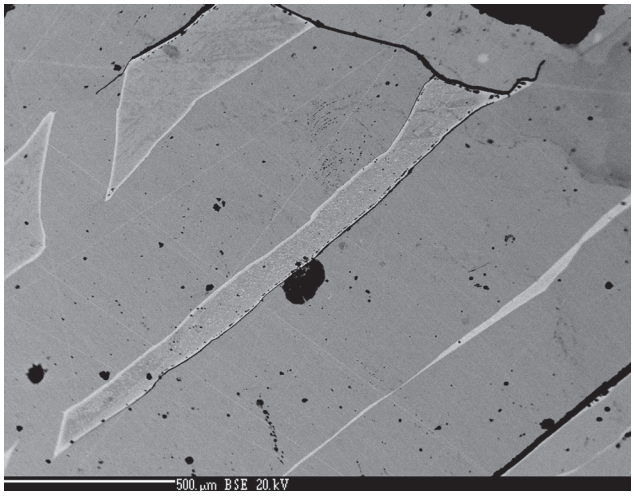

Fig. 7. Kamacite V. (BSE)

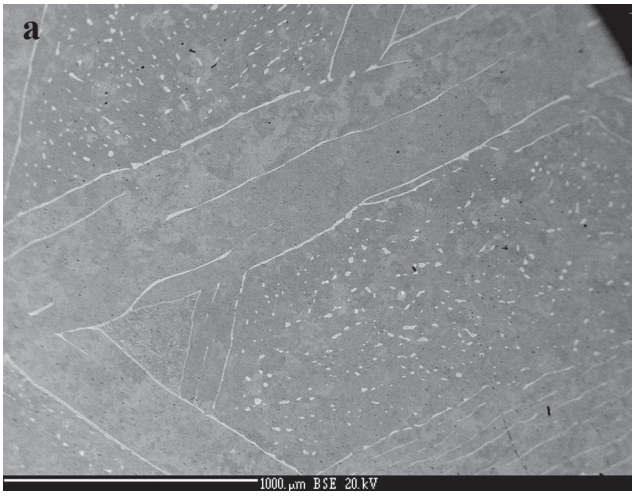

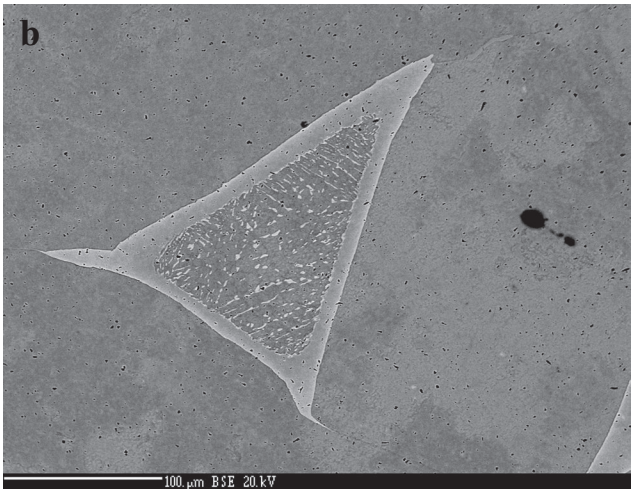

Fig. 8. a — Uniform arrangement of taenite grains; **b** — parallelly oriented grains of taenite in plessite texture (BSE).

significant dependencies were identified only between Co and Cu and only in the taenite (Fig. 9b,c,d), while in the kamacite the dependencies of Fe and Ni versus Co and Cu are missing. The negative correlation between Co and Ni in taenite documents the substitution of these two elements for one other. The negative correlation between Cu and Ni shows that Cu substitutes for Ni. In contrast, Fe is substituted by Co in the nickel irons structure with more similar ionic radius compared to Fe.

Depending on the total Ni content of the meteorite, kamacite formed at a temperature range of ~500–800 °C; the Ni content in the iron is increasing with a decreasing temperature. The presence of Widmanstätten patterns indicates that at higher temperatures the taenite crystals reach the size of tens of centimetres to 1 metre (Papike 1998). The Smolenice iron does not form visible Widmanstätten patterns in the cut, but after etching, these patterns are clearly visible and discernible. The Widmanstätten patterns have a classic appearance and copy the structural surfaces of the octahedrite. The complex and polyphase structures of the kamacite and taenite point to a complex decomposition of the original kamacite at temperatures below 400 °C (Yang et al. 1996, 1997a; Reuter et al. 1988; Papike 1998). The absence of Neumann's lines in the Smolenice meteorite proves that during its flight through space, no larger impact, or collision with another object happened.

Troilite (FeS) is a rare mineral in the Smolenice meteorite and forms oval grains of up to 3 mm in the kamacite (Fig. 10).

Table 1: Electron microprobe analyses of iron (kamacite) (in wt. %). n.a.=not analyzed.

No	Fe	Ni	Co	Cu	Ge	P	Si	Total
1	92.43	7.36	0.43	0.01	0.05	0.07	0.00	100.35
2	93.25	7.25	0.42	0.00	0.07	0.05	0.01	101.05
3	93.16	6.31	0.54	0.02	0.08	0.03	0.04	100.18
4	92.90	6.66	0.54	0.03	0.02	0.03	0.02	100.20
5	93.37	6.92	0.55	0.02	0.03	0.05	0.03	100.97
6	92.99	6.77	0.55	0.00	0.04	0.05	0.03	100.43
7	93.16	6.86	0.54	0.02	0.06	0.03	0.00	100.67
8	93.22	7.10	0.57	0.02	0.07	0.03	0.00	101.01
9	92.76	7.11	0.53	0.03	0.08	0.06	0.00	100.57
10	92.48	7.05	0.54	0.01	0.05	0.07	0.01	100.21
11	93.09	7.13	0.52	0.02	0.06	0.04	0.00	100.86
12	93.51	7.16	0.55	0.03	0.04	0.07	0.00	101.36
13	93.67	7.12	0.51	0.00	0.07	0.07	0.01	101.45
14	93.52	7.15	0.55	0.01	0.05	0.06	0.00	101.34
15	92.95	7.11	0.54	0.00	0.05	0.06	0.01	100.72
16	92.31	7.18	0.52	0.01	0.08	0.04	0.02	100.16
17	93.02	7.10	0.53	0.01	0.06	0.05	0.02	100.79
18	92.93	7.19	0.49	0.00	0.06	0.07	0.03	100.77
19	92.59	7.08	0.51	0.02	0.05	0.07	0.02	100.34
20	93.66	6.19	0.53	0.00	0.08	0.05	0.01	100.52
21	92.71	6.04	0.47	0.00	n.a.	n.a.	n.a.	99.22
22	91.20	6.88	0.47	0.00	n.a.	n.a.	n.a.	98.55
23	93.03	5.58	0.49	0.00	n.a.	n.a.	n.a.	99.10
24	93.15	5.47	0.47	0.02	n.a.	n.a.	n.a.	99.11
25	92.07	7.19	0.41	0.03	n.a.	n.a.	n.a.	99.70
26	91.59	7.22	0.40	0.01	n.a.	n.a.	n.a.	99.22
27	93.35	5.44	0.50	0.00	n.a.	n.a.	n.a.	99.29
28	92.97	5.97	0.49	0.00	n.a.	n.a.	n.a.	99.43
29	92.93	5.66	0.47	0.00	n.a.	n.a.	n.a.	99.06
30	94.08	5.16	0.47	0.02	n.a.	n.a.	n.a.	99.73
31	91.45	7.25	0.59	0.02	0.06	0.04	n.a.	99.41
32	92.44	7.26	0.55	0.01	0.07	0.05	n.a.	100.38
33	91.05	7.31	0.56	0.02	0.04	0.06	n.a.	99.04
34	91.09	7.09	0.57	0.02	0.06	0.07	n.a.	98.90
35	91.65	7.21	0.60	0.00	0.06	0.06	n.a.	99.58
36	93.18	5.89	0.61	0.00	0.06	0.02	n.a.	99.76
37	90.90	7.17	0.56	0.04	0.07	0.05	n.a.	98.79
38	91.33	7.16	0.60	0.00	0.08	0.06	n.a.	99.23
Min.	90.90	5.16	0.40	0.00	0.02	0.02	0.00	98.55
Max.	94.08	7.36	0.61	0.04	0.08	0.07	0.04	101.45
Mean	92.66	6.76	0.52	0.01	0.06	0.05	0.01	100.04
Std. dev.	0.83	0.64	0.05	0.01	0.02	0.01	0.01	0.81

Table 2: Electron microprobe analyses of taenite (in wt. %). n.a.=not analyzed.

No	Fe	Ni	Co	Cu	Ge	P	Si	Total
1	74.38	25.44	0.19	0.07	0.06	0.01	0.00	100.15
2	71.83	28.47	0.16	0.08	0.07	0.00	0.00	100.61
3	70.83	29.96	0.15	0.11	0.06	0.02	0.02	101.15
4	69.36	31.27	0.14	0.12	0.05	0.00	0.01	100.95
5	69.56	31.15	0.14	0.13	0.08	0.01	0.00	101.07
6	68.26	32.17	0.13	0.14	0.08	0.01	0.01	100.80
7	71.92	27.28	0.28	0.11	0.08	0.00	0.24	99.91
8	69.70	30.46	0.25	0.12	0.07	0.02	0.02	100.64
9	82.38	17.44	0.46	0.06	0.08	0.01	0.02	100.45
10	81.70	18.04	0.40	0.06	0.08	0.00	0.00	100.28
11	81.12	18.75	0.44	0.08	0.07	0.03	0.00	100.49
12	82.83	17.05	0.48	0.05	0.06	0.00	0.00	100.47
13	74.18	25.53	0.28	0.08	0.06	0.01	0.00	100.14
14	78.66	21.29	0.32	0.06	0.07	0.03	0.01	100.44
15	76.75	23.00	0.28	0.10	0.06	0.03	0.02	100.24
16	77.92	22.15	0.30	0.06	0.06	0.02	0.00	100.51
17	72.71	26.58	0.25	0.09	0.07	0.01	0.23	99.94
18	81.69	18.37	0.43	0.07	0.05	0.01	0.02	100.64
19	75.89	22.57	0.29	0.08	n.a.	n.a.	n.a.	98.83
20	77.35	21.60	0.26	0.05	n.a.	n.a.	n.a.	99.26
21	80.82	17.69	0.33	0.03	n.a.	n.a.	n.a.	98.87
22	74.11	24.60	0.24	0.07	n.a.	n.a.	n.a.	99.02
23	78.48	20.36	0.31	0.06	n.a.	n.a.	n.a.	99.21
24	77.20	21.83	0.26	0.07	n.a.	n.a.	n.a.	99.36
25	76.08	23.08	0.22	0.07	n.a.	n.a.	n.a.	99.45
26	75.86	24.02	0.23	0.05	n.a.	n.a.	n.a.	100.16
27	76.21	23.31	0.20	0.08	n.a.	n.a.	n.a.	99.80
28	76.77	23.03	0.20	0.05	n.a.	n.a.	n.a.	100.05
29	76.82	22.55	0.24	0.04	n.a.	n.a.	n.a.	99.65
30	73.49	26.48	0.33	0.11	0.06	0.01	n.a.	100.48
31	72.35	27.51	0.27	0.10	0.07	0.01	n.a.	100.31
32	70.87	28.55	0.29	0.12	0.07	0.01	n.a.	99.91
33	69.48	30.11	0.26	0.13	0.06	0.01	n.a.	100.05
34	70.67	28.83	0.29	0.10	0.06	0.01	n.a.	99.96
35	82.75	16.73	0.49	0.05	0.08	0.01	n.a.	100.11
36	72.09	27.80	0.32	0.10	0.07	0.00	n.a.	100.38
37	65.77	33.92	0.24	0.17	0.07	0.00	n.a.	100.17
38	76.04	23.23	0.37	0.09	0.07	0.02	n.a.	99.82
Min.	65.77	16.73	0.13	0.03	0.05	0.00	0.00	98.83
Max.	82.83	33.92	0.49	0.17	0.08	0.03	0.24	101.15
Mean	75.13	24.53	0.28	0.08	0.07	0.01	0.03	100.10
Std. dev.	4.48	4.69	0.09	0.03	0.01	0.01	0.07	0.58

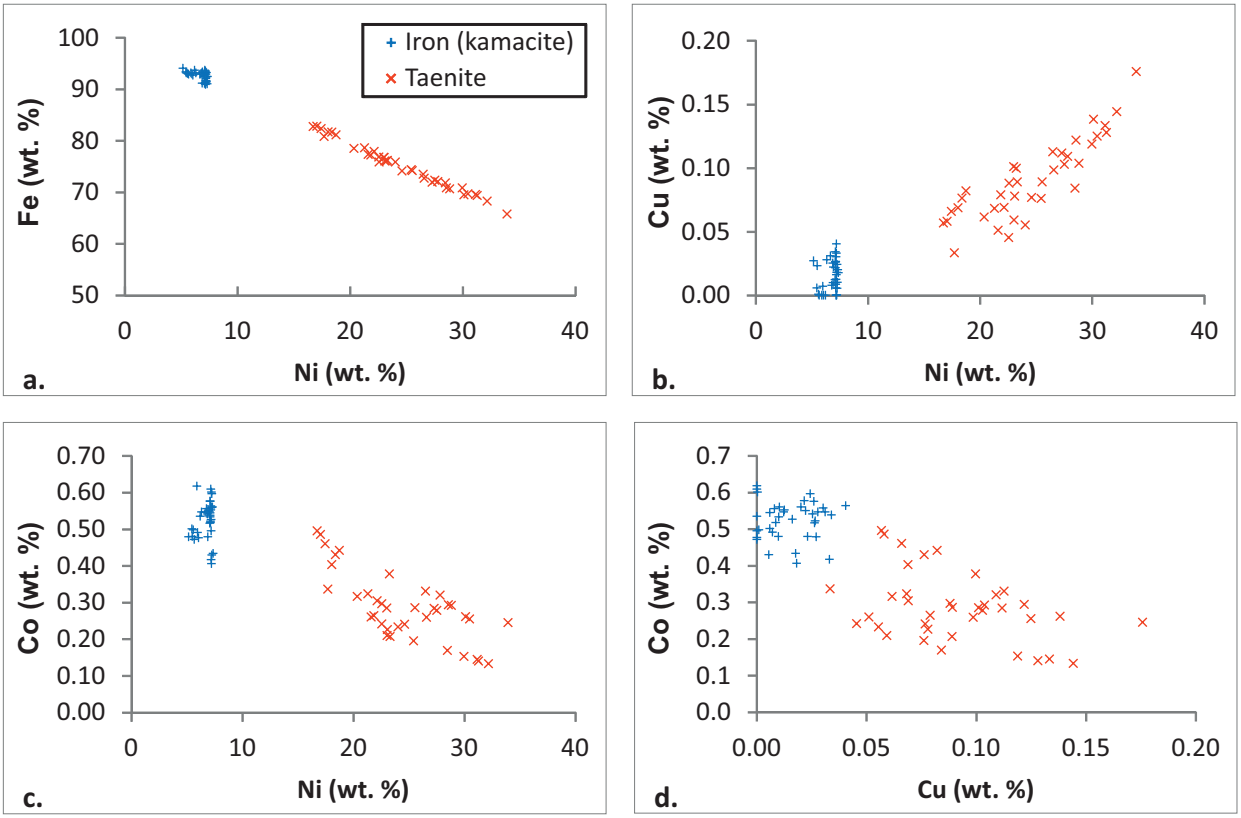

Fig. 9. a,b,c,d — Substitution diagrams in metals (kamacite, taenite).

The crystal-chemical formula of the troilite is $(Fe_{0.988–1.004}Cr_{0.008–0.015})_{\Sigma=0.988–1.008}S_{0.995–1.030}$ (normalized on 2 atoms). Among the admixtures, the Smolenice iron is characterized by an increased content of chromium, which is probably due to nano-exsolutions of daubréelite. This is indicated by very thin exotic lamellae of the daubréelite (Fig. 11). Average chemical composition of the troilite (in wt. %): Fe 62.38, S 36.13, Ni 0.01, Cu 0.02, Ge 0.06, Ga 0.01, Si 0.01, Cl 0.01, Ti 0.01, Σ 99.25. Chemical analyses of the troilite are shown in Table 3. Other measured chemical elements including Zn, Mn, Ga, Al, Ti, P, Si, and Cl are not listed in the table as their contents were below the detection limit.

Daubréelite ($Fe^{2+}Cr_2^{3+}S_4$) (Fig. 11) is a rare mineral in the Smolenice meteorite and was observed only in troilite as lamellae with a maximum width of 80 μm (Fig. 12). Very thin exsolution lamellae are also frequent with widths up to 0.8 μm (Fig. 13). The daubréelite lamellae are parallel to the cleavage of troilite. The crystal-chemical formula of daubréelite is $(Fe_{1.009–1.085}Ni_{0.000–0.002}Co_{0.000–0.001}Cu_{0.001–0.003}Mn_{0.019–0.023})_{\Sigma=1.028–1.114}Cr_{1.978–2.048}(S_4Cl_{0.000–0.003})$ (normalized on 4 atom of S). Electron microprobe analyses of daubréelite are presented in Table 4. The table does not include the measured elements Co, Zn, Ga, Al, Ti, P, Si, and Cl, which have contents below the detection limit. For this type of daubréelite found in troilite, an increased content of manganese (up to 0.42 wt. %=0.023 *apfu*) is typical. On the other hand, the increased concentrations of Cr are characteristic for troilite. Similar textures and exsolution lamellae of the daubréelite in troilite are known from various types of meteorites (e.g., Buchwald 1975; Rubin 1984; Olsen et al. 1988; Sarbas & Töpper 1993; Skála et al. 2000; Lin & El Goresy 2002). For daubréelite in troilite, the increased content of manganese is typical, and is known from both irons and EH chondrites (e.g., Rubin 1984, Sarbas & Töpper 1993, Lin & El Goresy 2002, etc.; Fig. 14). As shown in Fig. 14, the Mn contents in the Smolenice iron as well as in other irons where it occurs together with the troilite, are usually lower than in enstatite chondrites. This may be related to the nucleation of the troilite–daubréelite grains almost always dominated by troilite, which cannot accommodate Mn. The daubréelite, being a younger mineral, occurs in the form of exsolutions or lamellae.

Hydrated iron oxides are a product of surface weathering and usually do not penetrate deep into the meteorite. Oxidative iron alterations occur selectively along individual iron lamellae. Taenite appears to be more resistant to oxidation than kamacite (Fig. 15a,b). Oxidation products of terrestrial weathering penetrate along the fissures into troilite as well, being approximately perpendicular to the cleavage of troilite (Fig. 11).

The main mass of the Smolenice iron is slightly weathered. No limonite veinlets were detected in the meteorite under polarized light, nor in the electron microprobe. However, a small part of the iron meteorite is weathered on the surface and this part is typically less than 1 mm, but locally it penetrates up to several mm into the meteorite.

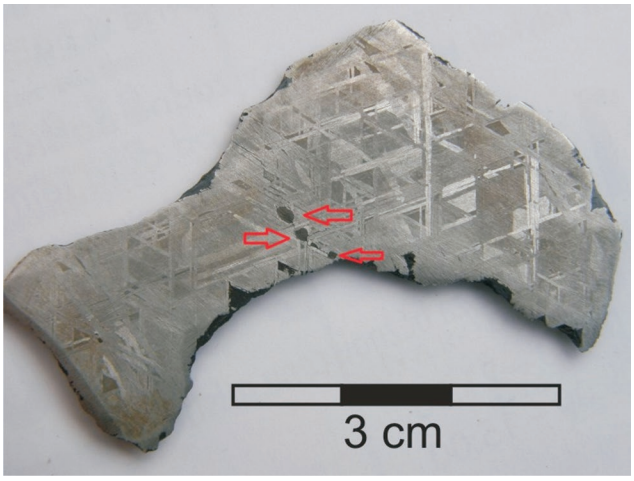

Fig. 10. Widmanstätten pattern in Smolenice. Three arrows show nodules of troilite (photo: S. Antalík).

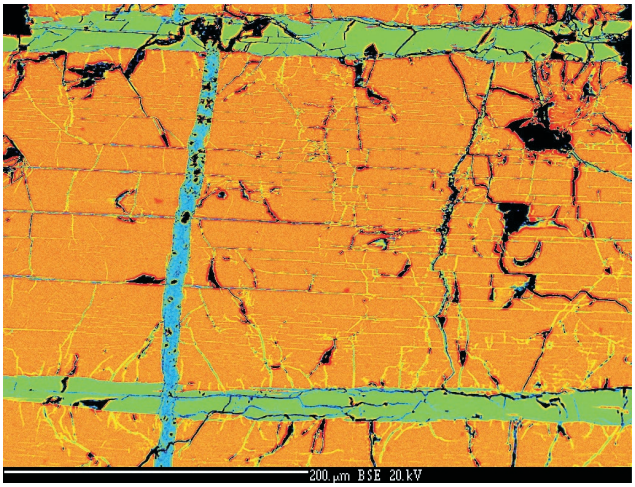

Fig. 11. Troilite (orange), daubréelite (green) and hydrated iron oxides (blue), (BSE).

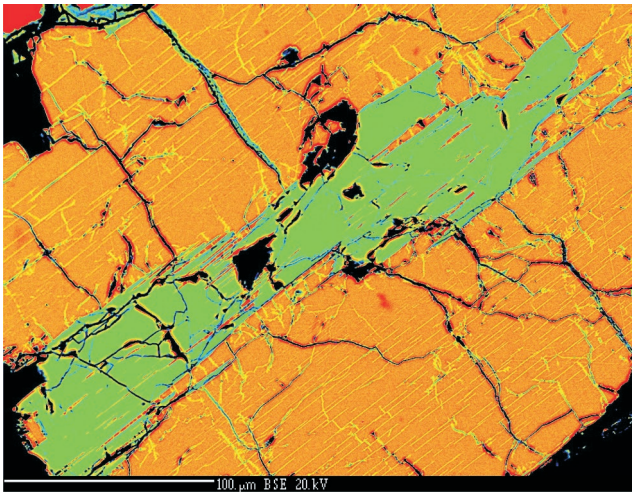

Fig. 12. Daubréelite inclusion (green) in troilite (orange), (BSE).

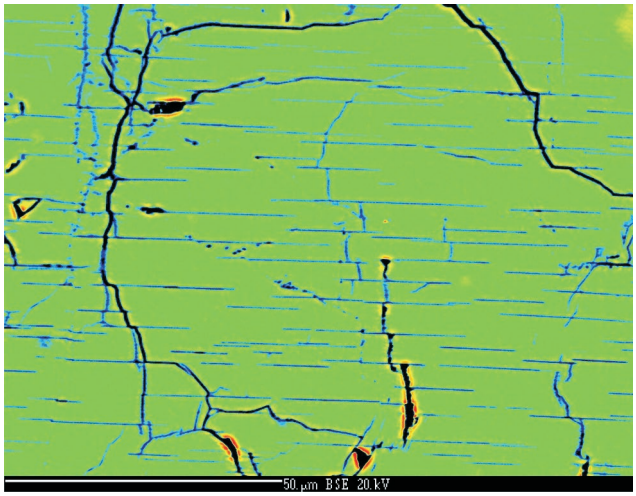

Fig. 13. Thin lamellae of daubréelite (blue) in troilite (green), (BSE).

Table 3: Electron microprobe analyses of troilite (in wt. %). n.a.=not analyzed.

No	Fe	Cr	Ni	Co	Cu	Ge	S	Total
1	62.19	0.73	0.00	0.02	0.01	0.06	35.86	98.87
2	61.58	0.77	0.02	0.02	0.00	n.a.	36.41	98.80
3	61.84	0.86	0.00	0.00	0.02	n.a.	36.30	99.02
4	61.67	0.61	0.00	0.02	0.01	n.a.	36.13	98.44
5	62.27	0.66	0.01	0.03	0.01	n.a.	36.28	99.26
6	62.35	0.69	0.01	0.01	0.01	n.a.	36.22	99.29
7	62.83	0.62	0.01	0.00	0.00	n.a.	36.21	99.67
8	62.48	0.75	0.02	0.00	0.03	n.a.	36.41	99.69
9	62.63	0.59	0.01	0.00	0.03	n.a.	35.79	99.05
10	62.72	0.48	0.00	0.00	0.01	n.a.	35.93	99.14
11	62.40	0.63	0.00	0.00	0.01	n.a.	36.16	99.20
12	62.32	0.61	0.00	0.01	0.02	n.a.	35.91	98.87
13	62.27	0.59	0.02	0.02	0.02	n.a.	36.06	98.98
14	62.92	0.67	0.00	0.01	0.03	0.06	35.95	99.64
15	63.14	0.60	0.01	0.00	0.02	0.05	36.30	100.12
Min.	61.58	0.48	0.00	0.00	0.00	0.05	35.79	98.44
Max.	63.14	0.86	0.02	0.03	0.03	0.06	36.41	100.12
Mean	62.37	0.66	0.01	0.01	0.02	0.06	36.13	99.20
Std. dev.	0.44	0.09	0.01	0.01	0.01	0.01	0.20	0.43

Table 4: Electron microprobe analyses of daubréelite (in wt. %). n.a.=not analyzed.

No	Fe	Mn	Ni	Cu	Ge	Cr	S	Total
1	19.78	0.38	0.03	0.03	0.07	35.63	43.29	99.21
2	19.36	0.38	0.01	0.04	0.06	34.82	43.41	98.08
3	19.06	0.38	0.04	0.03	0.00	35.83	43.16	98.50
4	19.06	0.34	0.00	0.03	0.00	35.94	43.41	98.78
5	19.03	0.40	0.03	0.02	0.00	35.64	43.04	98.16
6	19.98	0.36	0.02	0.05	0.00	34.93	42.27	97.61
7	19.41	0.38	0.00	0.05	0.00	35.41	43.38	98.63
8	19.13	0.40	0.00	0.06	0.00	35.19	43.03	97.81
9	19.38	0.40	0.00	0.03	0.00	35.16	42.99	97.96
10	19.25	0.40	0.00	0.05	0.00	35.43	43.12	98.25
11	19.34	0.40	0.00	0.01	0.00	35.20	42.89	97.84
12	19.09	0.40	0.00	0.04	0.00	35.48	42.99	98.00
13	19.34	0.42	0.00	0.02	0.00	35.22	43.11	98.11
Min.	19.03	0.34	0.00	0.01	0.00	34.82	42.27	97.61
Max.	19.98	0.42	0.04	0.06	0.07	35.94	43.41	99.21
Mean	19.32	0.39	0.01	0.04	0.01	35.38	43.08	98.23
Std. dev.	0.28	0.02	0.01	0.01	0.02	0.33	0.30	0.45

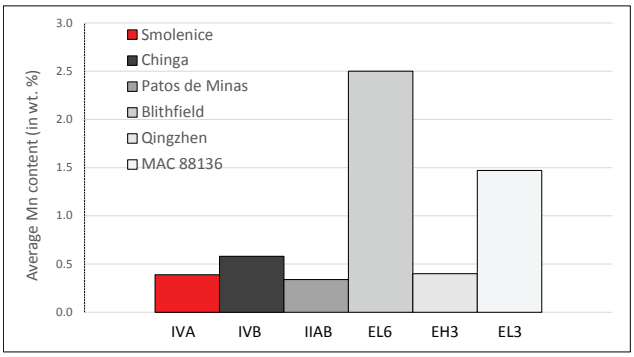

Fig. 14. Plot of Mn contents in daubréelites from various irons and enstatite chondrites. References: Irons — Smolenice (this study), Chinga (Plechov 2018), Patos de Minas (Varela et al. 2015); Enstatite chondrites — Blithfield (Rubin 1984), Quingzhen and MAC 88136 (both Lin & El Goresy 2002).

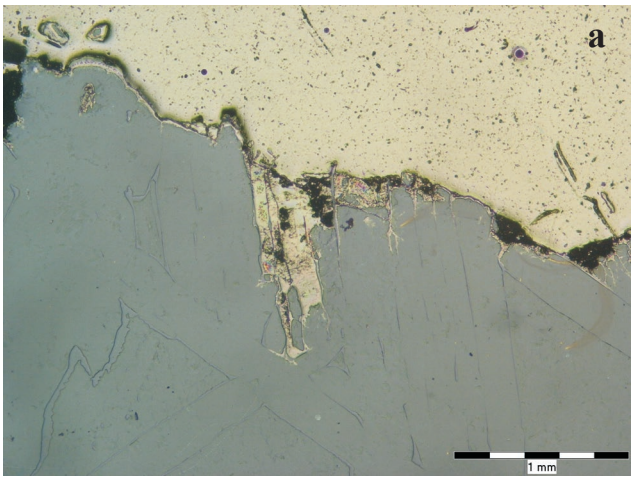

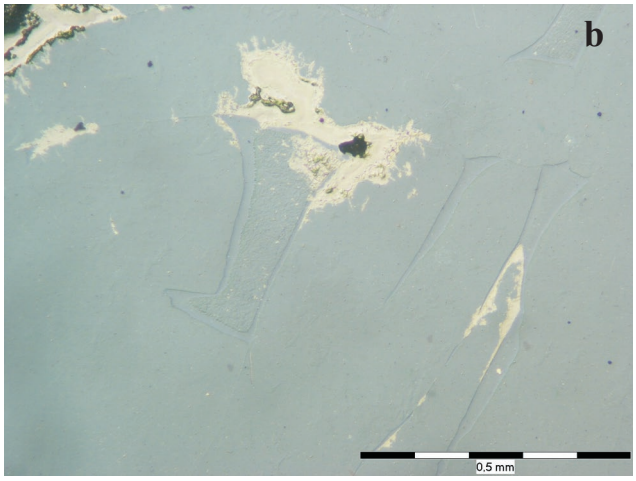

Fig. 15. a,b — Penetration of hydrated iron oxides (light grey) into iron (grey; polarized light).

Bulk geochemistry

The dominant composition of the two iron forms – kamacite and taenite, due to the low content of other minerals, also determines the chemical composition of the Smolenice meteorite in which the Fe+Ni content reaches 97.30–99.97 wt. %. Cobalt is present as a minor element (0.38 wt. %). All other studied elements are present only in trace amounts. The bulk analysis of the Smolenice meteorite (Table 5) is consistent with the meteoric iron of the IVA group (e.g., Wasson & Richardson 2001; McCoy et al. 2011; Benedix et al. 2014). The Smolenice meteorite was classified mainly on the basis of the Ni, Ga and Ge content (Figs. 16, 17), which clearly ranks it into the IVA group. Figure 18 shows a good match of the Ni content to Pt, Ir, Re, Au ratio in the Smolenice iron; according to the analyses it falls mostly into the central part of the field of this group of irons. Similarly, this is also true for the Ni/P ratio, where the Smolenice iron analysis falls into the centre of the IVA group analyses. By comparing the ratios of Au to other elements (Ga, Cr, W, Ir, As, Pt; Fig. 19), it is also possible to see a good match with the data for other IVA irons groups. Only the cobalt content has a small excess (Co:Au=3.8:1.19; Table 5), outside the main range of analyses, but similar excess of cobalt was also found in the irons Altonah (3.69:1.46) and Alvord (3.8:1.44; Buchwald 1975). However, the inclusion of the Smolenice meteorite in this group is unlikely due to the low Ga content of (1.80 μg/g) and the width of the kamacite lamellae, which is several times larger in the meteorites of this group (Hutchison 2006) than in Smolenice. When comparing

Table 5: Results of ICP-OES (Fe, Ni, Co, P, S – in wt. %) and ICP-MS (other elements – in μg/g) bulk analyses of the Smolenice meteorite. (LOQ is the limit of quantification).

Element	ICP-OES	LOQ
Fe	88.78	0.1
Co	0.378	0.0005
Ni	8.16	0.01
P	0.0485	0.005
S	<0.006	0.006
Total (%)	97.37	
B	<0.68	0.68
Cr	87.3	0.2
Cu	135.1	0.5
Zn	<5	5
Ga	1.8	0.05
Ge	<0.18	0.18
As	4.52	0.1
Mo	5.82	0.13
Ru	3.56	0.0025
Rh	0.897	0.003
Pd	4.12	0.015
Sn	1.53	0.03
W	0.565	0.07
Re	0.176	0.003
Ir	1.67	0.003
Pt	5.35	0.006
Au	1.19	0.04
Pb	<0.06	0.06

the Ni and Ir contents, the iron from Smolenice falls well within a relatively narrow field of IVA group irons analyses (Fig. 20), but also in the part characteristic of the analyses for the IIIAB, IIIF and IAB groups. However, other classification criteria such as the Ga, Ir and Ge contents, the kamacite lamellae width as well as the characteristic minerals for these groups exclude the possibility of it being classified as IVA. Extraterrestrial irons of the IVA group come from the bodies with

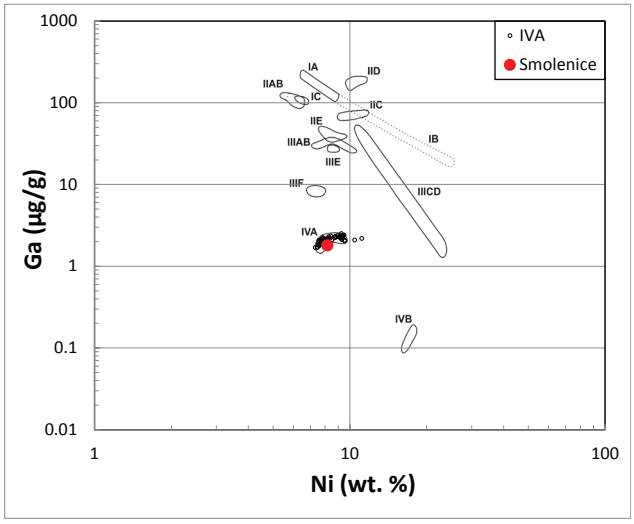

Fig. 16. Logarithmic plot of Ga vs. Ni of bulk composition of the Smolenice meteorite (the fields of iron groups are according to Scott & Wasson 1975).

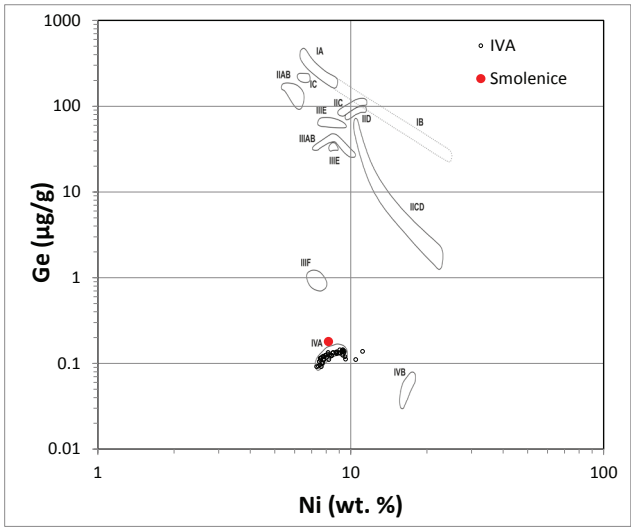

Fig. 17. Logarithmic plot of Ge vs. Ni of bulk composition of iron meteorites (the fields of iron groups are according to Scott & Wasson 1975). Points of IVA field show analyses of irons from this group.

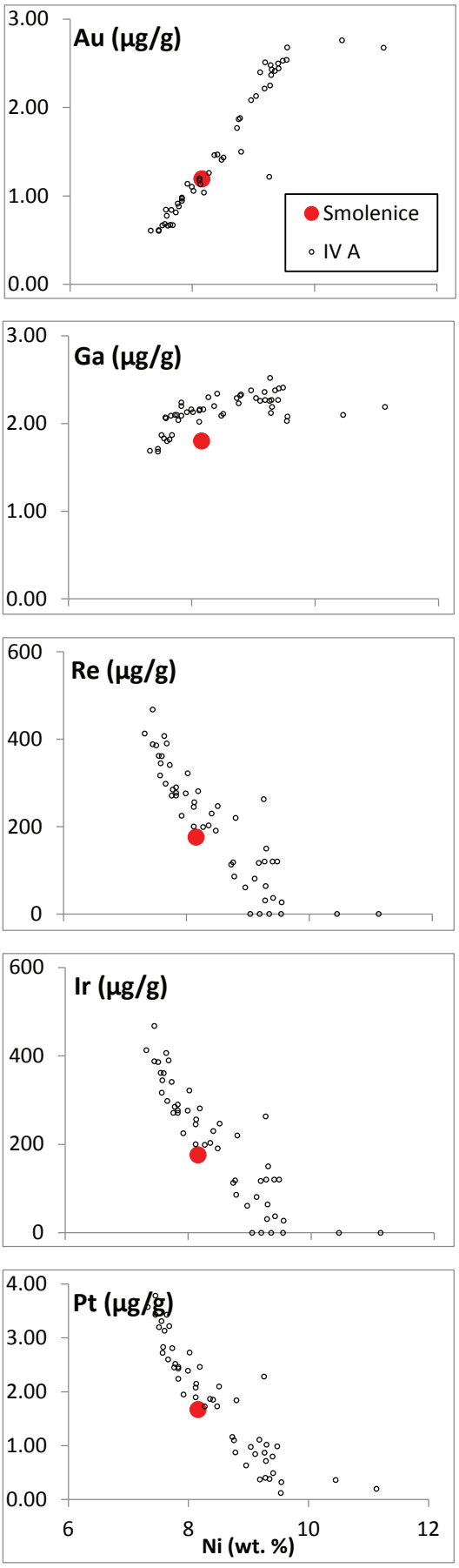

Fig. 18. Comparison of chemical composition of the Smolenice meteorite with 47 irons of IVA group (Wasson & Richardson 2001). Selected elements versus Ni.

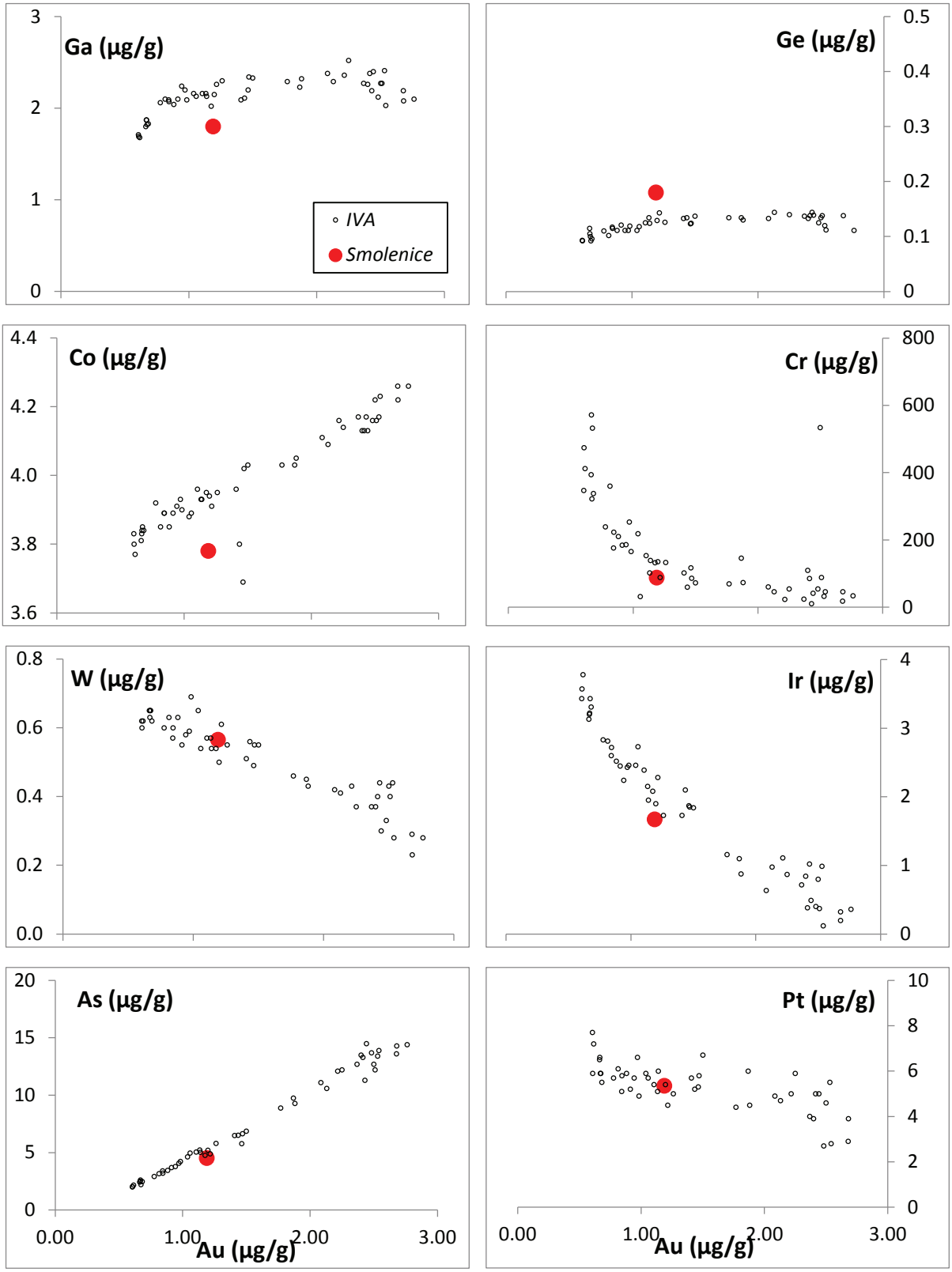

Fig. 19. Comparison of chemical composition of the Smolenice meteorite with 47 irons of IVA group (Wasson & Richardson 2001). Selected elements versus Au.

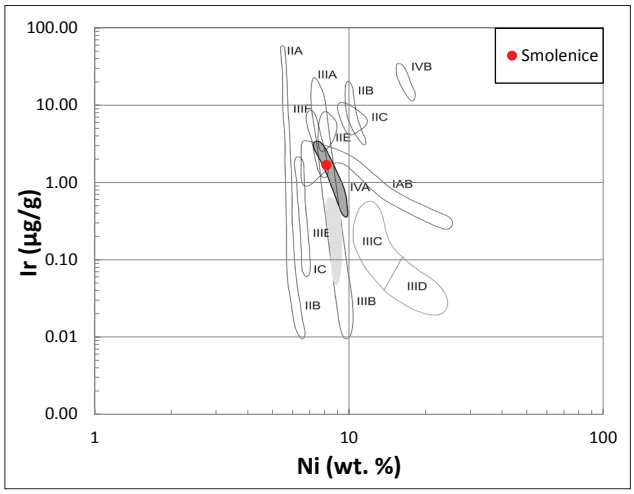

Fig. 20. Logarithmic plot of Ir vs. Ni of bulk composition of the Smolenice meteorite (the fields of iron groups are according to Scott & Wasson 1975).

a radius of 8–49 km (Haack et al. 1990), or 10–27 km (Yang et al. 1997b) and the cooling rate was 11–500 °C/Ma (Haack et al. 1990), or 40–325 °C/Ma (Yang et al 1997b).

Radionuclides

Two kinds of radionuclides can be found in meteorites. The first group is represented by primordial radionuclides (e.g., ^{235}U, ^{238}U, ^{232}Th and their decay products). The second group includes cosmogenic radionuclides produced by interaction of cosmic-ray particles with meteoroids during their orbits in space. We focus on cosmogenic radionuclides, mainly on long-lived ones (^{14}C – half-life of 5730 yr and ^{26}Al – half-life of 0.717 Myr), as the fall of the Smolenice meteorite was not observed and therefore all short-lived radionuclides might have already decayed during its stay at the earth surface. All these radionuclides have been produced in iron meteorites by galactic cosmic-ray protons and secondary neutrons on target nuclei of iron, nickel and aluminium.

Aluminium-26 has been frequently studied in stone and iron meteorites because it decays by positron emission accompanied by characteristic gamma-rays of 1808.65 keV, which makes its detection by a non-destructive gamma-ray spectrometry feasible (Povinec et al. 2015b). The measured ^{26}Al activity in the Smolenice fragment is 3.12±0.24 dpm/kg, close to the saturation level. This value also clearly demonstrates that the analysed fragment is a meteorite. This value is consistent with the expected production rate of ^{26}Al from Fe (Masarik & Reedy 1994). Leya & Masarik (2009) give a slightly higher production rate of 3.7 dpm/kg, which would then suggest moderate shielding. When compared with other iron meteorites (and after appropriate corrections for self-absorption of gamma-rays in the sample), this value fits well within the expected meteoroid radius of 30±10 cm, if the terrestrial age of Smolenice is about 10 kyr (Lavrukhina & Ustinova 1990; Ammon et al. 2009).

As ^{14}C is a pure beta-emitter with maximum energy of beta-electrons of only 156 keV, the measurements were carried out by AMS. We obtained the result of 0.95±0.02 dpm/kg and we can compare this to the production-rate values for ^{14}C from Fe of 4.0 and 3.0 dpm/kg given by Masarik & Reedy (1994) and Leya & Masarik (2009). Using these values, we can calculate the terrestrial age directly from decay of ^{14}C from the production rate ratios for ^{14}C/^{26}Al. Propagating the errors, this results in a terrestrial age of 9.6±0.7 ky based on Leya & Masarik (2009) or 12.0±0.7 ky from the production ratios of Masarik & Reedy (1994). We can therefore estimate the terrestrial age to be in the range of 9 to 13 ky. Improved estimates may be obtained by additional measurement of ^{10}Be in Smolenice to use this as a shielding correction (e.g., Jull et al. 2010).

Potassium-40 in iron meteorites (because of its low content) is more likely to be produced by cosmic rays, while in stone meteorites it belongs to primordial radionuclides (Lavrukhina & Ustinova 1990). The measured ^{40}K activity in the Smolenice meteorite is 22.5±4.9 dpm/kg, however, the ^{40}K gamma-ray peak (1460.8 keV) is also found in the spectrometer background, therefore special care is required during spectra evaluation (Povinec 2018). As we cannot rule out possible contamination of the Smolenice meteorite by terrestrial ^{40}K, more work is needed to solve the problem of the origin of ^{40}K (e.g., by ^{40}K analysis of other iron meteorites).

Conclusions

In 2012 a suspected iron meteorite weighing 13.95 kg was found in south-western Slovakia, near the town of Smolenice. Based on the Widmanstätten patterns, chemical and mineral composition and other features it was confirmed as such. The Smolenice meteorite is composed predominantly of iron. Taenite lamellae, troilite nodules and daubréelite veinlets and parallel intergrowths occur rarely. According to Ir, Ga, Ni and Ge contents, the Smolenice iron can be classified into the IVA group. Based on average kamacite bandwidths (0.22 mm), this iron is a fine octahedrite (Of).

Analyses of cosmogenic radionuclides (^{26}Al and ^{14}C) indicate that the radius of the Smolenice meteorite could be 30±10 cm and its terrestrial age of 11±2 kyr.

Acknowledgements: S. Farsang acknowledges the F. A. Paneth Trust Meteorite Award of the Royal Astronomical Society. This work was supported by the Slovak Research and Development Agency under the contract Nr. APVV-0516-10, Nr. APVV-18-0065 and Nr. APVV-15-0050 and VEGA Agency of the Ministry of Education, Science, Research and Sport of the Slovak Republic under the contract Nr. 1/0151/19 and 1/0891/17. A.J. Timothy Jull also acknowledges support by the European Union and the State of Hungary, co-financed by the European Regional Development Fund in the project of GINOP-2.3.2-15-2016-00009 'ICER'. The authors thank P. Bačík for editorial handling of the paper and M. Szurgot and B.A. Hofmann for constructive reviews of the paper.

References

Ammon K., Masarik J. & Leya I. 2009: New model calculations for the production rates of cosmogenic nuclides in iron meteorites, *Meteorit. Planet. Sci.* 44, 485–503.

Benedix G.K., Haack H. & McCoy T.J. 2014: Iron and stony-iron meteorites. In: Holland H. & Turekian K. (Eds.): Treatise on Geochemistry 1. *Elsevier*, 267–285.

Buchwald V.F. 1975: Handbook of Iron Meteorites. Vol. 1. Iron meteorites in General. *University of California Press*, Berkeley, 1–243.

Frost M.J. 1965: Kamacite plate with estimation in octahedrites. *Mineral. Mag.* 35, 640–642.

Haack H., Rasmussen K.L. & Warren P.H. 1990: Effects of regolith/megaregolith insulation on the cooling histories of differentiated asteroids. *J. Geophys. Res.* 95, 5111–5124. https://doi.org/10.1029/JB095iB04p05111

Hutchison R. 2006: Meteorites. A Petrologic, Chemical and Isotopic Synthesis. Cambridge Planetary Science. *Cambridge University Press*, Cambridge, 1–506.

Jull A.J.T., Donahue D.J., Cielaszyk E. &Wlotzka F. 1993: ^{14}C terrestrial ages and weathering of 27 meteorites from the southern high plains and adjacent areas (USA). *Meteoritics* 28, 188–195.

Jull A.J.T., McHargue L.R., Bland P.A., Greenwood R.C., Bevan A.W.R., Kim K.J., Giscard M.D., LaMotta S.E. & Johnson J.A. 2010: Terrestrial ^{14}C and ^{14}C-^{10}Be ages of meteorites from the Nullarbor, Australia. *Meteorit. Planet. Sci.* 45, 1271–1283. https://doi.org/10.1111/j.1945-5100.2010.01289.x

Kováčik A., Sýkora I., Povinec P.P. & Porubčan V. 2012: Non-destructive gamma-spectrometry analysis of cosmogenic radionuclides in fragments of the Košice meteorite. *J. Radioanal. Nucl. Chem.* 293, 339–345. https://doi.org/10.1007/s10967-012-1667-4

Kováčik A., Sýkora I. & Povinec P.P. 2013: Monte Carlo and experimental efficiency calibration of gamma-spectrometers for non-destructive analysis of large volume samples of irregular shapes. *J. Radioanal. Nucl. Chem.* 298, 665–672. https://doi.org/10.1007/s10967-013-2509-8

Lavrukhina A.K. & Ustinova G. K. 1990: Meteorites – probes of cosmic-ray variations. *Nauka*, Moscow, 1–264.

Leya I. & Masarik J. 2009: Cosmogenic nuclides in stony meteorites revisited. *Meteorit. Planet. Sci.* 44, 1061–1086. https://doi.org/10.1111/j.1945-5100.2009.tb00788.x

Lin Y. & El Goresy A. 2002: A comparative study of opaque phases in Qingzhen (EH3) and MacAlpine Hills 88136 (EL3): Representatives of EH and EL parent bodies. *Meteorit. Planet. Sci.* 37, 577–599. https://doi.org/10.1111/j.1945-5100.2002.tb00840.x

Masarik J. & Reedy R. 1994: Effects of bulk composition on nuclide production processes in meteorites. *Geochim. Cosmochim. Acta* 58, 5307–5317. https://doi.org/10.1016/0016-7037(94)90314-X

McCoy T.J., Walker R.J., Goldstein J.I., Yang J., McDonough W.F., Rumble D., Chabot N.L., Ash R.D., Corrigan C.M., Michael J.R. & Kotula P.G. 2011: Group IVA irons: New constraints on the crystallization and cooling history of an asteroidal core with a complex history. *Geochim. Cosmochim. Acta* 75, 6821–6843. https://doi.org/10.1016/j.gca.2011.09.006

Olsen E.J., Huss G.I. & Jarosewich E. 1988: The Eagle, Nebraska enstatite chondrite (EL6). *Meteoritics* 23, 379–380.

Papike J.J. (Ed.) 1998: Planetary materials. *Rev. Mineral. Geochem.* 36, 1–864.

Plechov P. 2018: FMM Certificate 2018-33-9 (https://www.fmm.ru/images/2/28/FMM_Certificate_2018-33-9.pdf) 7.12.2018.

Povinec P.P. 2018: New ultra-sensitive radioanalytical technologies for new science. J. *Radioanal. Nucl. Chem.* 316, 893–931. https://doi.org/10.1007/s10967-018-5787-3

Povinec P.P., Sýkora I., Porubčan V. & Ješkovský M. 2009: Analysis of ^{26}Al in meteorite samples by coincidence gamma-ray spectrometry. *J. Radioanal. Nucl. Chem.* 282, 805–808. https://doi.org/10.1007/s10967-009-0211-7

Povinec P. P., Masarik J., Sýkora I., Kováčik A., Beňo J., Laubenstein M. & Porubčan V. 2015a: Cosmogenic radionuclides in the Košice meteorite: Experimental investigations and Monte Carlo simulations. *Meteorit. Planet. Sci.* 50, 880–892. https://doi.org/10.1111/maps.12380

Povinec P. P., Laubenstein M., Ferrière L., Brandstätter F., Sýkora I., Masarik J., Beňo J., Kováčik A., Topa D. & Koeberl C. 2015b: Cosmogenic radionuclides and mineralogical properties of the Chelyabinsk (LL5) meteorite: What do we learn about the meteoroid? *Meteorit. Planet. Sci.* 50, 272–286. https://doi.org/10.1111/maps.12419

Reuter K.B., Williams D.B. & Goldstein J.I. 1988: Low temperature phase transformations in the metallic phases of iron and stony–iron meteorites. *Geochim. Cosmochim. Acta* 52, 617–626. https://doi.org/10.1016/0016-7037(88)90323-7

Rubin A. E. 1984: The Blithfield meteorite and the origin of sulfide–rich, metal–poor clasts and inclusions in brecciated enstatite chondrites. *Earth Planet. Sci. Lett.* 67, 273–283. https://doi.org/10.1016/0012-821X(84)90167-5

Sarbas B. & Töpper W. 1993: Mn, Manganese. In: Gmelin Handbook of Inorganic and Organometallic Chemistry. 8th edition. *Springer*, Berlin, 1–180.

Scott R.D. & Wasson J.T. 1975: Classification and properties of iron meteorites. *Rev. Geophys. Space Phys.* 13, 4, 527–546.

Skála R., Frýda J. & Sekanina J. 2000: Mineralogy of the Vicenice octahedrite. *J. Czech Geol. Soc.* 45, 1–2, 175–192.

Varela M.E., Sylvester P., Souders K., Saavedra M. & Zucolotto M.E. 2015: Patos de Minas: A compositional study of sulphides, schreibersite and cohenite. In: *46th Lunar Planet. Sci. Conf.*, 1503.

Wasson J.T. & Richardson J.W. 2001: Fractionation trends among IVA iron meteorites: Contrast with IIIAB trends. *Geochim. Cosmochim. Acta* 65, 951–970. https://doi.org/10.1016/S0016-7037(00)00597-4

Yang C.-W., Williams D.B. & Goldstein J.I. 1996: A revision of the Fe–Ni phase diagram at low temperatures (<400 °C). *J. Phase Equilibria* 17, 522–531. https://doi.org/10.1007/BF02665999

Yang C.-W., Williams D.B. & Goldstein J.I. 1997a: Low–temperature phase decomposition in metal from iron, stony–iron and stony meteorites. *Geochim. Cosmochim. Acta* 61, 2943–2956. https://doi.org/10.1016/S0016-7037(97)00132-4

Yang C.-W., Williams D.B. & Goldstein J.I. 1997b: A new empirical cooling rate indicator for meteorites based on the size of the cloudy zone of the metallic phases. *Meteorit. Planet. Sci.* 32, 423–429. https://doi.org/10.1111/j.1945-5100.1997.tb01285.x